Copyright © 1975 American Telephone and Telegraph Company
THE BELL SYSTEM TECHNICAL JOURNAL
Vol. 54, No. 2, February 1975
Printed in U.S.A.

Analysis of Specially Doped Varactors for Direct Frequency Tripling

By S. V. AHAMED

(Manuscript received July 11, 1974)

Specially doped ($N = N_0/\sqrt{x}$) varactors offer a cubic relation between voltage and charge. Frequency tripling is thus possible without an idler frequency excitation at twice the input frequency. Here we have investigated a frequency tripler from 2.115 to 6.345 GHz without an idler frequency at 4.23 GHz, thus hopefully reducing the cost and complexity of the tripler.

The results from such varactors indicate that, although frequency tripling is possible over a wide band, the efficiency and power-handling capacity are considerably lower than conventional frequency tripling with abrupt junction varactors excited at 4.23 GHz. The impedance matching is harder for these specially doped varactors, even though the mechanical construction is greatly simplified.

I. INTRODUCTION

The varactor fabrication technique recently evolved is a notable beneficiary of the IMPATT developments. Such a transfer of technology from IMPATT to varactors[1] has resulted in diodes with a zero bias capacitance of 7.7 pF, a breakdown voltage of 160 V, and a series resistance of 0.66 ohm. These diodes have been utilized in the construction of a coaxial frequency doubler yielding 8.2 W[1] at 3990 mHz and 80-percent efficiency. Further, if these diodes are used for frequency tripling, they yield about 10 W[1] at 6.345 GHz and 72- to 76-percent efficiency. When the doping density is also controlled (as is done in high-low-high profile IMPATT's), it is possible to generate varactor diodes with any predefined relation between the charge and the voltage across the varactor.

Conventional frequency tripling studied by Penfield and Rafuse[2] asserts the presence of an idler frequency excitation at twice the input frequency to mix with the input frequency, thus creating a third harmonic voltage. In the proposed tripler, the doping density is adjusted to directly convert the power at incident frequency to power at

the third harmonic. This particular doping requirement (derived in the appendix) can be relatively easily achieved by the technique used in controlling[3,4] the doping densities of high-low and high-low-high profiles for IMPATT's and for voltage variable capacitors. The concept of varying[5] the doping density for tuning diodes has been reviewed by Norwood and Shatz.[6] The capacitance of P-n junctions has been studied by Chang.[7,8] This paper reports on the study of the efficiency, power capacity, bandwidth, and impedance characteristics of triplers built from varactors formed by the special doping distribution. Computed and experimental data from conventional triplers using an abrupt junction varactor and an idler frequency excitation are also presented to provide a bench mark for comparison.

II. FREQUENCY-TRIPLING MECHANISM

In the abrupt junction varactor, the instantaneous voltage V and charge q are related as

$$(V - V_0) = \alpha(q)^2, \tag{1}$$

giving rise to second harmonic voltages from the exciting frequency charges and currents. Third and fourth harmonic voltages are also generated, and if the currents at these frequencies are suppressed, then stable frequency doubling results. To achieve a third harmonic voltage, a second harmonic (idler) current is essential, and that is the well-established basis of conventional frequency tripling.[2]

Now consider a varactor in which the instantaneous voltage and charge are related as

$$(V - V_0) = \alpha(q)^3, \tag{2}$$

thereby giving rise to third harmonic voltages resulting from charges and currents at the exciting frequency. Stable frequency tripling is possible even if second harmonic currents are not present.

The doping density that leads to such a voltage-charge relation and the corresponding capacitance-voltage relationship is derived in the appendix, Section A.1.

III. DIODE CHARACTERIZATION

The breakdown voltage, the zero bias capacitance per unit area, the depletion layer width, and the series resistance are all influenced by the doping density. These parameters may be calculated if the doping densities at finite distance from the junction are known from the basic requirements that yield the voltage-charge relationship (2) (see appendix). Further, these parameters in turn critically affect the input and output powers, impedances, and the efficiency of the tripler. Only if the diode can be fabricated with existing technology, and if the

input and output characteristics of the overall tripler are compatible with the existing technique of impedance matching, do we have a successful tripler design. Three important characteristics influencing the circuit performance of the diode are: (*i*) the breakdown voltage V_b, (*ii*) the zero bias capacitance C_0, and (*iii*) its series resistance R_s. The breakdown voltage is limited by the maximum electric intensity that the first layer* can withstand. Equation (12) yields the breakdown voltage at different doping densities for various first-layer thicknesses (see Fig. 1). The zero bias capacitance C_0 and the series resistance R_s are inversely related to each other to the first degree of approximation.† Hence, if a typical zero bias capacitance of 7.5 pF is assumed, then the series resistance at different doping densities may be computed. These curves are also shown in Fig. 1.

IV. RESULTS OF THE SIMULATION

4.1 Diode simulation study

Simulation of the results presented in the appendix yields the data necessary to study the performance of the diode from circuit and systems considerations. While the diode is tripling the frequency directly, the circuit parameters may be determined as follows: An impedance across the output is assumed to dissipate a known power; the current and charge at the triple frequency in the diode are derived; and the fundamental frequency current and charge required to sustain the output charge and current are evaluated at different values of static biasing charges across the junction from the fundamental voltage-charge relationship, eq. (2). The limits of the charge excursion across the junction during one cycle at fundamental frequency excitation are compared against the minimum and maximum charges‡ which the diode is capable of withstanding. Only if these minimum and maximum limits are not violated can the diode generate the known power. The input impedance is computed by the voltage-charge relationship at the fundamental frequency. The efficiency and bandwidth are determined by evaluating the losses in the diode at the first and third harmonic frequencies, and by incrementing the input frequency from its nominal value at 2.115 GHz. The various equations governing the distribution of charge, impedances, and efficiency are discussed in the appendix, Section A.3.

---

* For analysis, the doping profile may be approximated by a series of layers in which the doping density is held constant.

† The exact computation of these parameters has been programmed in the simulation developed for the analysis on the HIS 600 computer.

‡ This is known from the value of the breakdown voltage V_b and α in eq. (2). The minimum charge is zero.

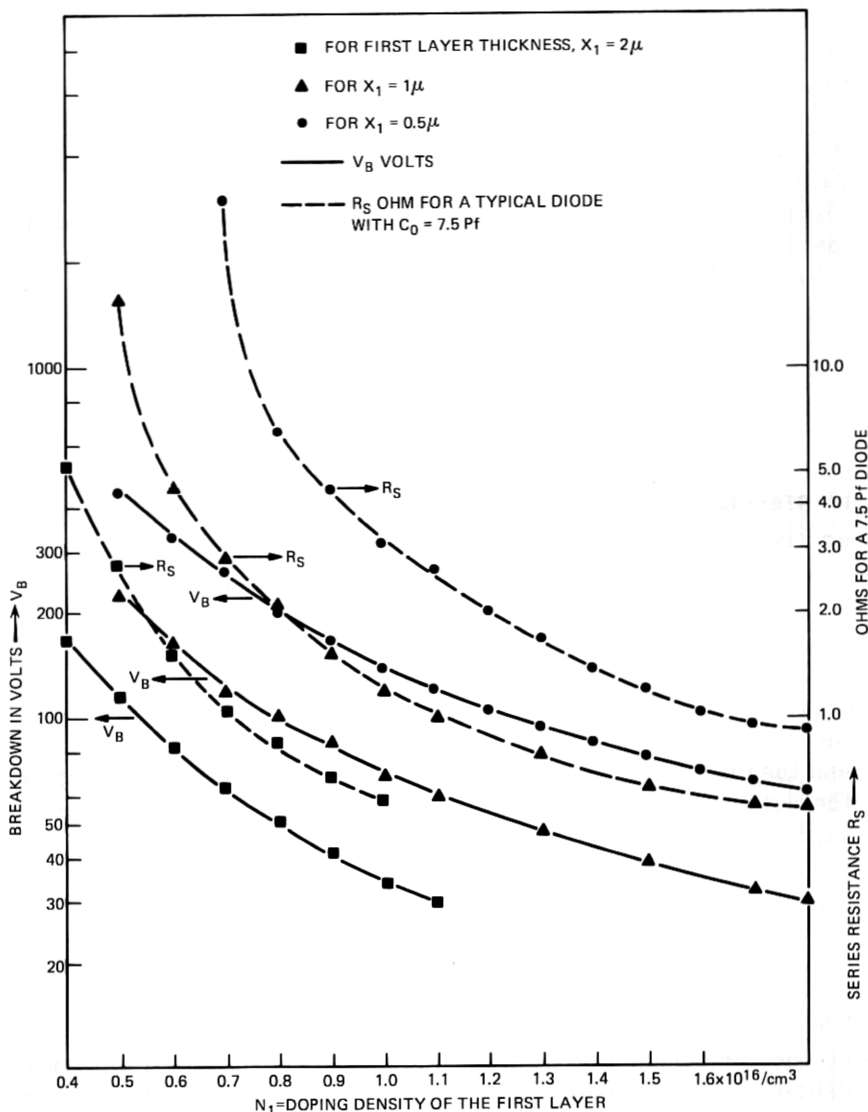

Fig. 1—V_B, R_S characteristics for $N = N_0X^{-\frac{1}{2}}$.

4.2 Single-chip diode performance curves

A single-chip diode can be designed from the basic relationships presented in appendix Sections A.1 and A.2. The diode characteristics, α, V_b, and R_s (discussed in the appendix), lead to the performance curves of the tripler. Figures 2 and 3 depict the performance of two typical diodes with zero bias capacitances of 7.5 pF ($\alpha = 0.61 \times 10^{32}$,

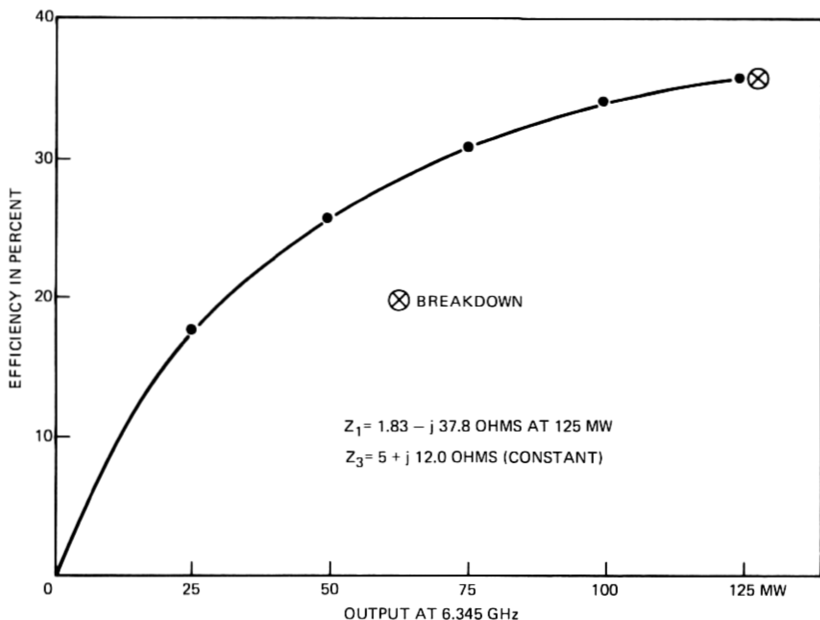

$\alpha = 0.61 \times 10^{32}$, $V_B = 58$ V, $R_S = 1.04$ OHMS

DEPLETION LAYER WIDTH = 4.05μ, DIAMETER = 6.39 MILS

LAYER	THICKNESS	DOPING DENSITY
1	2μ	$0.74 \times 10^{16}/cm^3$
2	0.5	$0.446 \times 10^{16}/cm^3$
3	0.5	$0.410 \times 10^{16}/cm^3$
4	0.5	$0.382 \times 10^{16}/cm^3$
5	0.5	$0.359 \times 10^{16}/cm^3$
6	0.5	$0.339 \times 10^{16}/cm^3$

Fig. 2—Efficiency characteristic of single-chip 7.5-Pf varactor diode.

$V_b = 58$ V, $R_s = 1.04$ ohms) and 15 pF ($\alpha = 0.762 \times 10^{31}$, $V_b = 58$ V, and $R_s = 0.54$ ohm).

4.3 Double-stacked diode performance curves

When two single chips are stacked in series across the 2.115-GHz supply, the breakdown voltage and the resistance double, while the capacitance halves. The resistance of each chip is, however, inversely proportional to its capacitance. Hence, a 7.5-pF-stacked diode made from two 15-pF diodes would have a breakdown voltage of 116 V and $R_s = 1.08$ ohms.

The performance curves of two diodes with a zero bias capacitance of 7.5 pF ($\alpha = 0.152 \times 10^{32}$, $V_b = 116$ V, and $R_s = 1.08$ ohms) and 10 pF ($\alpha = 0.643 \times 10^{31}$, $V_b = 116$ V, and $R_s = 0.84$ ohm) are shown in Figs. 4 and 5.

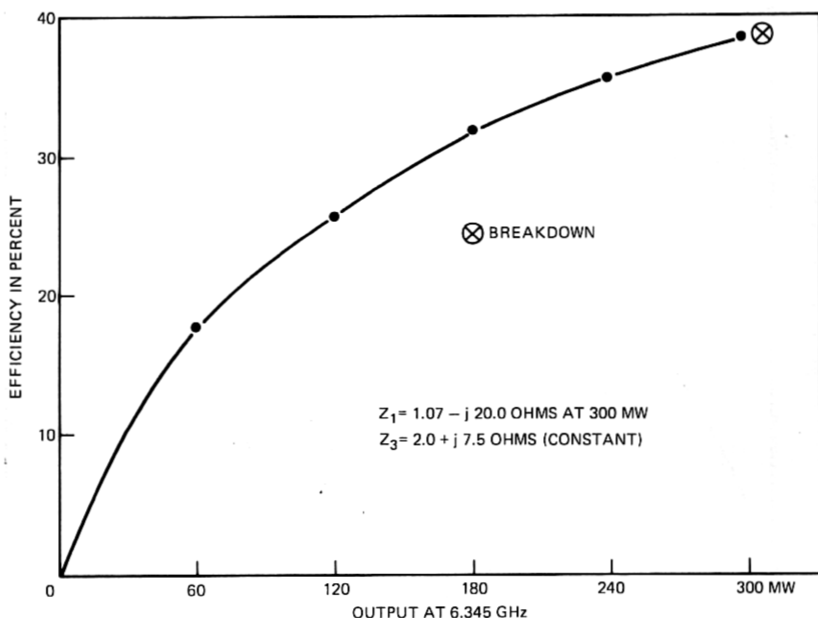

$\alpha = 0.754 \times 10^{31}$, $V_B = 58$ V, $R_S = 0.543$ OHMS

DEPLETION LAYER WIDTH = 4.05μ, DIAMETER = 9.04 MILS

LAYER	THICKNESS	DOPING DENSITY
1	2μ	$0.74 \times 10^{16}/\text{cm}^3$
2	0.5	$0.446 \times 10^{16}/\text{cm}^3$
3	0.5	$0.410 \times 10^{16}/\text{cm}^3$
4	0.5	$0.382 \times 10^{16}/\text{cm}^3$
5	0.5	$0.359 \times 10^{16}/\text{cm}^3$
6	0.5	$0.339 \times 10^{16}/\text{cm}^3$

Fig. 3—Efficiency characteristic of single-chip 15.0-Pf varactor diode.

4.4 Triple-stacked diode performance curves

Two typical diodes having zero bias capacitances of 5 and 7.5 pF yield the efficiency-output characteristics shown in Figs. 6 and 7. Three single-chip diodes with zero bias capacitance, $C_0 = 15$ pF, are stacked to obtain the first 5-pF, 174-V, 1.62-ohm diode, and three chips each with 22.5 pF, 58 V, and 0.38 ohm constitute the second diode.

4.5 Effect of changing the doping density

The diode may also be fabricated by altering the concentration densities in the various layers of the diode. The value of N_0 is computed from N_1, the first layer doping density. In most of the simulation presented thus far, the value of N_1 was held at $0.74 \times 10^{16}/\text{cm}^3$. It

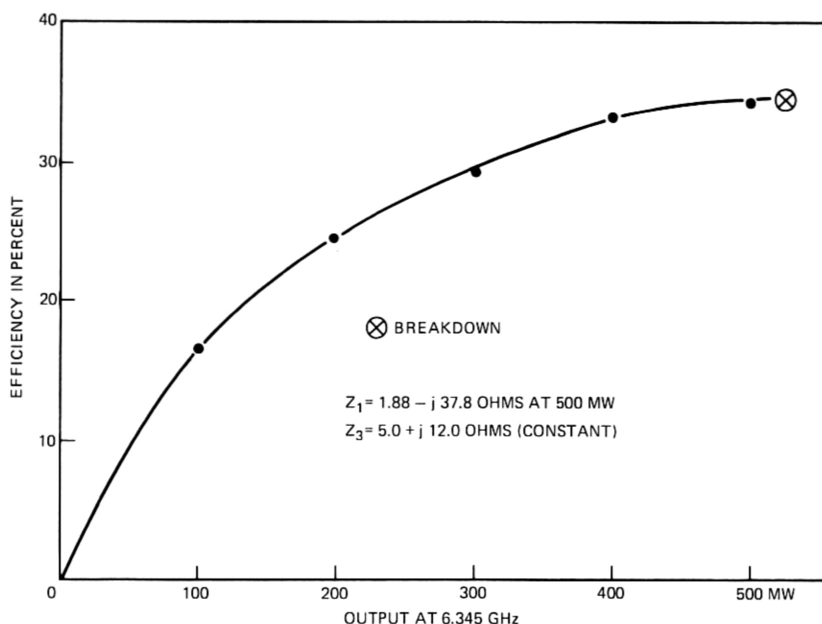

Fig. 4—Efficiency characteristics of 7.5-Pf stacked diode.

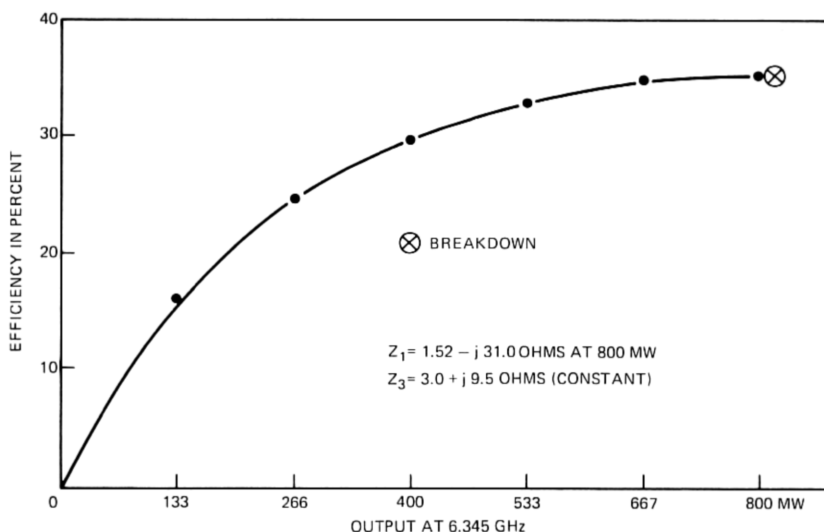

Fig. 5—Efficiency characteristics of 10-Pf stacked diode with $N_1 = 0.74 \times 10^{16}/\text{cm}^3$.

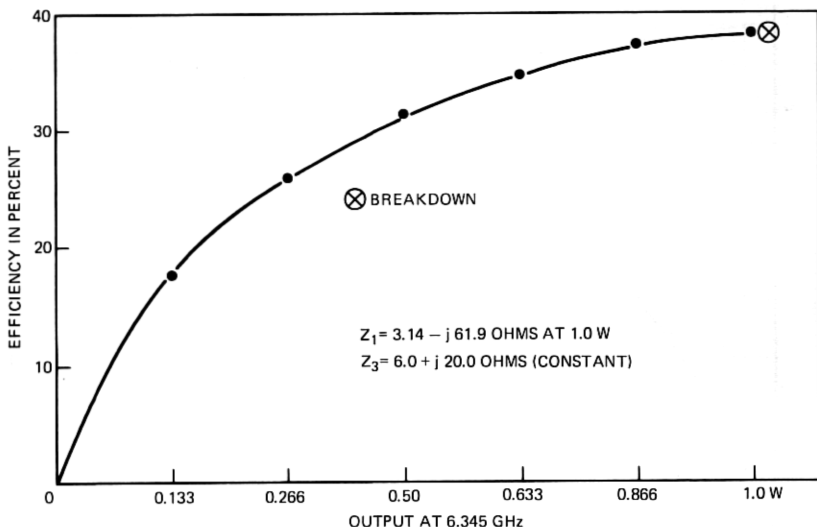

Fig. 6—Efficiency characteristics of 5-Pf triple-stacked diode.

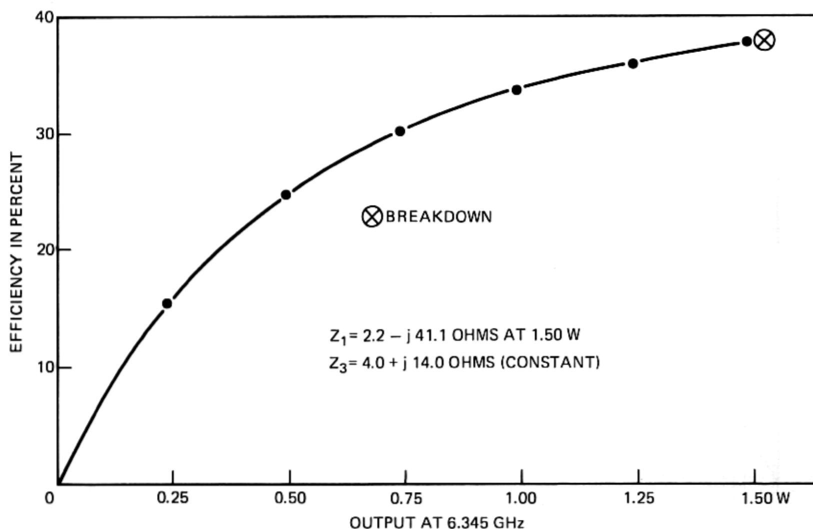

Fig. 7—Efficiency characteristics of 7.5-Pf triple-stacked diode.

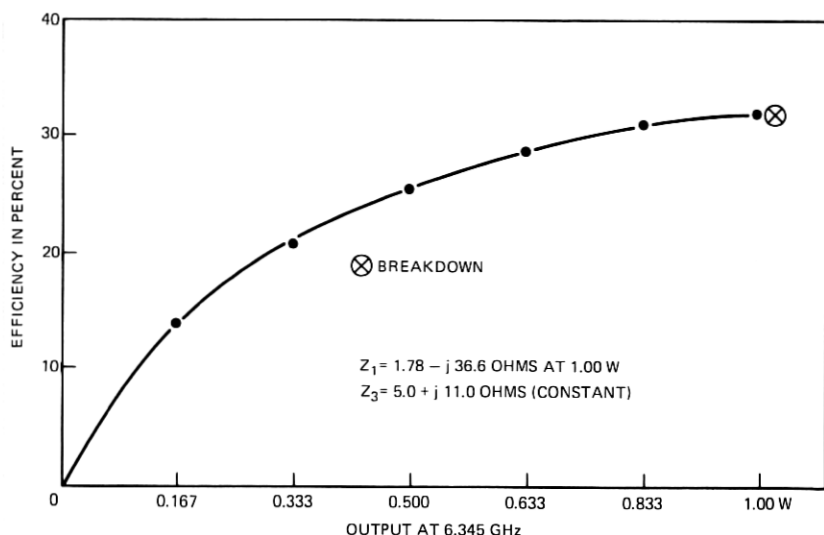

$\alpha = 0.643 \times 10^{31}$, V_B = 149 V, R_S = 1.09 OHMS

STACKED DIODE OBTAINED BY TWO 20–Pf DIODES EACH HAVING DEPLETION LAYER WIDTH = 5.27μ, DIAMETER = 11 MILS, 8 LAYERS AS FOLLOWS:

LAYER	THICKNESS	DOPING DENSITY
1	2μ	$N_1 = 0.64 \times 10^{16}/\text{cm}^3$
2	0.5	$0.386 \times 10^{16}/\text{cm}^3$
3	0.5	$0.355 \times 10^{16}/\text{cm}^3$
4	0.5	$0.330 \times 10^{16}/\text{cm}^3$
5	0.5	$0.310 \times 10^{16}/\text{cm}^3$
6	0.5	$0.294 \times 10^{16}/\text{cm}^3$
7	0.5	$0.279 \times 10^{16}/\text{cm}^3$
8	0.5	$0.267 \times 10^{16}/\text{cm}^3$

Fig. 8—Efficiency characteristic of 10-Pf stacked diode.

was found by trial that a certain compromise between power and efficiency could be reached at this doping level. However, for the sake of completeness, results with doping densities of $N_1 = 0.64 \times 10^{16}/\text{cm}^3$ and $N_1 = 0.84 \times 10^{16}/\text{cm}^3$ are also presented in Figs. 8 and 9 for a 10-pF diode obtained by stacking two 20-pF diodes.

V. DISCUSSION OF SIMULATED RESULTS

5.1 Power-handling capacity

When the doping density at contact is in the region of 0.7 to $0.8 \times 10^{16}/\text{cm}^3$, the breakdown voltage for specially doped varactors is about 50 percent* lower than that of the abrupt junction varactor.

---

* For $N_1 = 0.75 \times 10^{16}/\text{cm}^3$, $N_0 = 0.75 \times 10^{19}$ with $x_1 = 2\ \mu$ and $V_b = 60.57$ V for specially doped varactor, whereas $V_b = 89.3$ V for abrupt junction varactor. E_{max} is 44×10^4 V/cm.

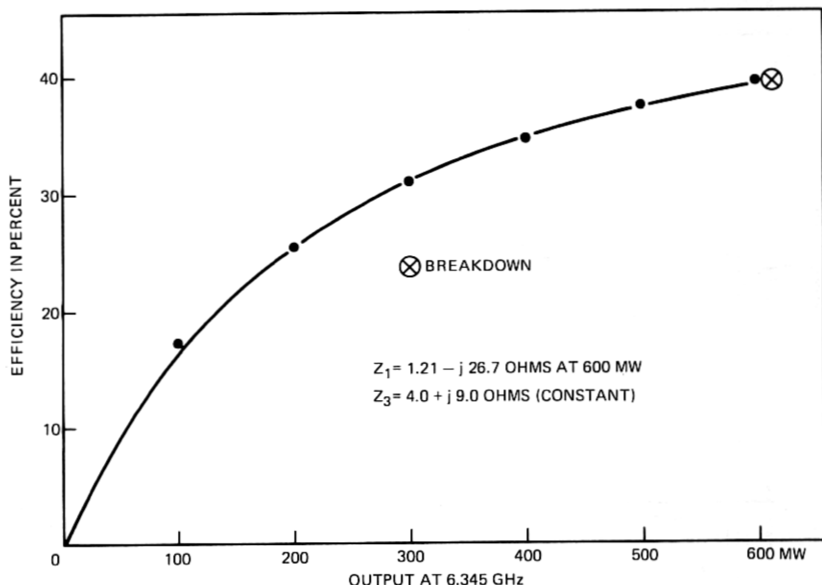

$\alpha = 0.643 \times 10^{31}$, $V_B = 93$ V, $R_S = 0.65$ OHMS
STACKED DIODE OBTAINED BY TWO 20–Pf DIODES EACH HAVING DEPLETION LAYER WIDTH OF 3.22μ, DIAMETER = 10 MILS, 4 LAYERS AS FOLLOWS:

LAYER	THICKNESS	DOPING DENSITY
1	2μ	$N_1 = 0.84 \times 10^{16}/\text{cm}^3$
2	0.5	$0.506 \times 10^{16}/\text{cm}^3$
3	0.5	$0.466 \times 10^{16}/\text{cm}^3$
4	0.5	$0.434 \times 10^{16}/\text{cm}^3$

Fig. 9—Efficiency characteristics of 10-Pf stacked diode with $N_1 = 0.84 \times 10^{16}/\text{cm}^3$.

Thus, the total power-handling capacity is severely impaired. Further, the solution of cubic equations relating the charge q_1 at the fundamental frequency and the third harmonic charge q_3 leads to the lowest value of q_1 being approximately six times q_3, whereas the corresponding solutions in the conventional tripler with an idler yield the charges $q_3 : q_2 : q_1$ at the fundamental, the idler, and the third harmonic frequencies to be approximately in the proportion of 1:1.37:2.27. This further reduces the power that can be obtained from the tripler. For a triple-stacked, specially doped varactor, the breakdown voltage is 174 V and the power output is 1.5 W. For a triple-stacked, abrupt junction varactor with an idler circuit, the breakdown voltage is 262 V, and power output is 12.0 W, as shown in Fig. 10.

5.2 Efficiency

The specially doped varactor resistance, being a sum of the resistances of the various layers approximating the ($N = N_0 x^{-\frac{1}{2}}$) profile, is

higher than that of the abrupt junction diode. This is especially the case if the depletion layer is wide and if the doping density farther away from the junction is much less than the doping density of the first layer. The efficiency is thus adversely affected. Further, the proportion of charges q_1 and q_3 entail a relatively higher magnitude of q_1 than its corresponding value for a conventional tripler. The fundamental frequency current is much higher, thereby increasing the dissipation in the series resistance of the diode.

While the efficiency of the tripler is limited to a range of 30 to 40 percent with an output of 1 to 1.5 W (see Figs. 2 to 9) at 6.345 GHz, the efficiency (see Fig. 10) of a triple-stacked, abrupt junction tripler is well into the 70- to 76-percent range with an output of 8 to 10 W. For this particular diode, the zero bias capacitance C_0 is 5.0 pF, the breakdown voltage V_b is 262 V, and the series resistance is 0.97 ohm.

5.3 Impedances

The higher value of q_1 required to sustain q_3 reduces the real component of impedance to low values. Most of the power exchange takes place when the inductive component of the output is matched to tune out the average elastance of the diode, and the capacitive component

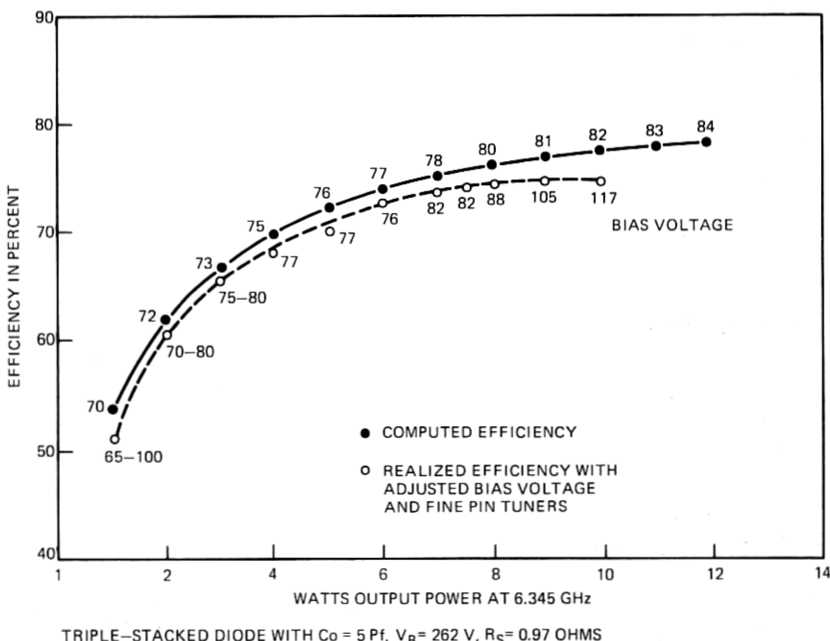

Fig. 10—Efficiency characteristic of a conventional tripler with abrupt junction and idler frequency excitation at 4.23 GHz ($N = 0.76 \times 10^{16}/cm^3$).

of the input impedance becomes approximately three times the inductive component of the output impedance. Typically, the output and input impedances of a triple-stacked diode with a zero bias capacitance of 7.5 pF, breakdown voltage of 174 V, and a series resistance of 1.14 ohms while delivering 1.5 W at 6.345 GHz are $(4 + j14)$ and $(2.21 - j41.5)$ ohms. These impedances are typical of the diode with special doping.

5.4 Bandwidth

The lack of an idler circuit makes this tripler reasonably broadbanded. When the output frequency is varied by approximately 700 mHz, the real component of the input impedance remains at 2.21 ohms, and the imaginary component varies from 43.6 to 38.9 ohms. A 70-mHz variation causes a change from 41.3 to 40.7 ohms. In comparison, the conventional tripler* undergoes a change from 7.28 to 5.71 ohms (real component) and 39.53 to 43.18 ohms (imaginary component) when the output frequency is changed by 35 mHz on either side of this nominal value at 6.345 GHz. Figures 11a and 11b depict the experimentally determined bandwidth characteristics of a conventional tripler at 8- and 5-W output.

5.5 Effect of diode design variations

The reduction for N_1 from $(0.74 \text{ to } 0.64) \times 10^{16}/\text{cm}^3$ increases the breakdown voltage from 116 to 148.6 V, thus increasing the power from 800 mW to 1 W. Also, the accompanying increase in resistance from 0.84 to 1.09 ohms reduces the efficiency from 35 to 32 percent. Converse results occur when the doping density of the first layer is increased from $(0.74 \text{ to } 0.84) \times 10^{16}/\text{cm}^3$. The power-handling capacity is reduced to 600 mW, and efficiency increases to about 40 percent owing to reduced resistance of 0.648 ohm.

VI. EXPERIMENTAL VERIFICATION

In view of the results obtained from the computer simulation, the experimental investigation has been limited. Instead of actually constructing diodes with the prespecified doping densities, the high-low-high profile IMPATT junction has been used with the high doping density region almost etched out to leave a steeply descending concentration level. This concentration approximates the ideal $(N = N_0/\sqrt{x})$ relation, thus making the voltage-charge relation dominated by a cubic term.

---

* These results are obtained by the analysis of a triple-stacked, abrupt junction varactor into a zero bias capacitance of 5 pF, breakdown voltage of 262 V, and a series resistance of 1.03 ohms while delivering 6 W into an impedance of $10 + j21.6$ ohms. The variation accounts for the variation in idler circuit impedance because of a change in frequency.

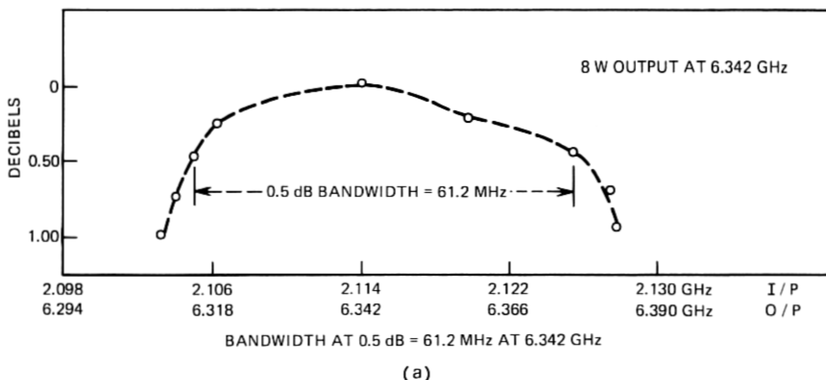

(a)

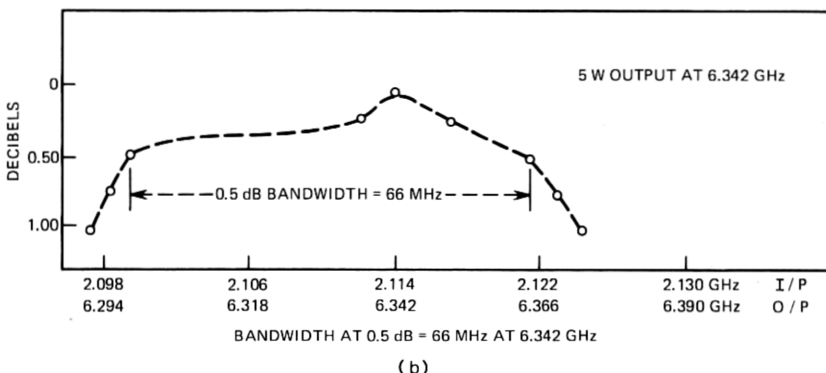

(b)

Fig. 11—0.5-dB bandwidth data of the conventional tripler built with an abrupt junction diode having $C_0 = 5$ Pf, $V_b = 262$ V, and $R_S = 0.97$ ohm.

Experiments with such varactors for direct frequency tripling have confirmed that the power output is in the region of 100 to 400 mW, depending on the size and breakdown voltage. The efficiency has been in the region of 15 to 27 percent, indicating the lossy components. These diodes prefer to slip into the conventional frequency-tripling mode by utilizing any adjoining tuner circuits for circulating the idler frequency currents. Impedance matching is a sizable problem, causing frequent burnouts of the diodes.

VII. CONCLUSIONS

From power, efficiency, and impedance design considerations, the specially doped varactor without an idler frequency excitation cannot compete with the conventional abrupt junction varactor excited at idler frequency. The decrease in complexity of construction (owing to lack of idler) does not offset the reduction in power-handling capacity, the low efficiency, or the poor impedance. However, for a wideband,

low-power-signal frequency tripling, the specially doped varactor outperforms the abrupt junction varactor. The analytical study presented here, though not completely complemented by experimental results, indicates the power levels, impedances, and efficiencies one may expect from such specially doped GaAs varactors.

VIII. ACKNOWLEDGMENT

The author thanks H. Seidel for the numerous discussions during the analysis and simulation of these specially doped varactors as triplers. R. M. Ryder provided excellent review of the manuscript, and J. C. Irvin supplied the diodes for experimental verification.

APPENDIX

A.1 Basic space-charge equations governing the distribution of the potential

The electric potential ψ and space-charge density $[\rho = eN(x)]$ are related* by Poisson equation in the region

$$\frac{d^2\psi}{dx^2} = -\frac{eN(x)}{\epsilon}, \tag{3}$$

where e is the electronic charge ($= 1.602 \times 10^{-19}$ coulombs), ϵ = permittivity of the region [presently, $\epsilon = 110.75 \times 10^{-12}$ F/m, which is the product of $\epsilon_0 (= 8.854 \times 10^{-12}$ F/m) and the relative permittivity $\epsilon_r (= 12.5$ for GaAs)], and finally $N(x)$ is the doping density in concentration per cubic meter, with x being measured in meters.

If the doping density is adjusted to vary by a specific relation such as

$$N(x) = N_0 x^n, \tag{4}$$

then it is possible to evaluate the exponent n to obtain the desired eq. (2) in Section II. Integrating (3) twice, we have

$$\psi = \frac{N_0 e x^{n+2}}{\epsilon(n+1)(n+2)} + C_1 x + C_2,$$

or

$$V = \psi - c_2 = \frac{N_0 e x^{n+2}}{\epsilon(n+1)(n+2)} + C_1 x, \tag{5}$$

when $x = x_d$ = the depletion layer width, then $V = V_a$, the applied voltage, and

$$\frac{dV}{dx} = 0 \quad \text{at} \quad x = x_d,$$

---

* This basic relationship is discussed in most standard books such as *Microwave Semiconductor Devices and their Circuit Application,* edited by H. A. Walton, New York: McGraw-Hill, 1969.

and

$$c_1 = \frac{N_0 e x_d^{n+1}}{\epsilon(n+1)} \tag{6}$$

$$V_a = \frac{N_0 e x_d^{n+2}}{\epsilon(n+2)} \tag{7}$$

$$x_d = \frac{\epsilon V_a (n+2)^{(1/n+2)}}{N_0 e}. \tag{8}$$

Now Q, charge per unit area, may be evaluated as

$$Q = \epsilon \left[\frac{dv}{dx} \right]_{x=0} = \frac{N_0 e}{n+1} \left[\frac{\epsilon(n+2)}{N_0 e} V_a \right]^{(n+1/n+2)}.$$

If $n = -\frac{1}{2}$, $(n + 1/n + 2) = \frac{1}{3}$, and we have

$$\begin{aligned} Q &= 2\sqrt[3]{(\tfrac{3}{2}) \cdot \epsilon (N_0 e)^2}\, V_a^{\frac{1}{3}} \text{ coulomb/m}^2 \\ &= \alpha_0 (V - V_0)^{\frac{1}{3}}, \end{aligned} \tag{9}$$

where V_0 is the normal contact potential, being about 1.2 V for GaAs contacts. Hence, if the doping density is adjusted to approximate $N = N_0 x^{-\frac{1}{2}}$, we would have the necessary charge-voltage relationship [eq. (2)] for direct tripling of frequency. Here, $\alpha = (\alpha_0 A)^{-3}$, where A is the cross-sectional area of the diode in square meters. Thus,

$$\alpha = 0.02941 \times 10^{36}/(N_0^2 A^3). \tag{9a}$$

A.2 Diode characterization

A.2.1 Breakdown voltage

The maximum voltage gradient permitted for GaAs contacts at various doping densities is known. Therefore, the breakdown voltage for an $N = N_0 x^{-\frac{1}{2}}$ doping distribution at various doping densities may be plotted from the equation

$$V_b = 4 \times 10^{16} [E(N_0)]^3 N_0^{-2} \text{ V}. \tag{10}$$

If the doping density is to be exactly $N = N_0/\sqrt{x}$, then N reaches an infinite value at $x = 0$. To eliminate this situation, the first layer doping density is held as N_1 (per cubic meter) and the value of N_0 is calculated as $N_0 = 0.707\, N_1 x_1^{\frac{1}{2}}$, where x_1 indicates the width of the first layer in meters. The doping densities for the mth adjoining layer is calculated as

$$N_m = N_0 \left(\sum_{i=1}^{m-1} X_i + X_m/2 \right)^{-\frac{1}{2}}. \tag{11}$$

In essence, the doping density distribution is approximated by a series of layers with different doping densities, and the value of the doping

density at the center of each layer corresponds to the necessary distribution of $N = N_0 x^{-\frac{1}{2}}$.

The values of V_b may be plotted against the first layer doping density N_1 for different values of the first layer thicknesses (x_1). Equation (10) now assumes the form

$$V_b = 8 \times 10^{16} [E(N_1)]^3 N_1^{-2} x_1^{-1} \text{ V}, \tag{12}$$

where $E(N_1)$ is in volts per meter, N_1 is in impurity concentration per cubic meter, and x_1 is in meters (see Fig. 1).

A.2.2 Diode resistance

This may be calculated by adding the resistances of the various layers. The resistivities at different values of doping densities are well known,[9] and the total resistance* may be calculated as

$$R_s = R_c + \sum_{i=1}^{i=m} \frac{\rho(N_i) l_i}{A}, \tag{13}$$

where R_c is the contact resistance inversely proportional to the area of cross-section A, $\rho(N_i)$ is the resistivity of the ith layer with a doping density of N_i, and l_i is the width of the ith layer.

A.2.3 Summary of equations

Depletion layer width is

$$x_d = 102.53 \times 10^{-4} N_0^{-\frac{2}{3}} (V + V_0)^{\frac{2}{3}} \text{ m}. \tag{14}$$

Maximum voltage gradient is

$$E_{\max} = 0.02924 \times 10^{-4} N_0^{\frac{2}{3}} (V + V_0)^{\frac{1}{3}} \text{ V/m}. \tag{15}$$

Capacitance per unit area is

$$C = 1.079 \times 10^{-16} N_0^{\frac{2}{3}} (V + V_0)^{-\frac{1}{3}} \text{ F/m}^2. \tag{16}$$

Charge per unit area is

$$Q = 3.2394 \times 10^{-16} N_0^{\frac{2}{3}} (V + V_0)^{\frac{1}{3}} \text{ cb/m}^2. \tag{17}$$

A.3 Circuit performance of the diode as a tripler

A.3.1 Loss-less-varactor formulations

The voltages and charges in the basic relationship

$$(V - V_0) = \alpha q^3 \tag{2}$$

---

* This formulation is correct at a negligible depletion layer width. In practice, the depletion layer is swept during each cycle at the input frequency. In the conventional tripler analysis, the reduction of loss because of sweeping of the epitaxial layer enhanced the efficiency by 2 to 4 percent, while the triple-stacked abrupt junction diode (see Fig. 10) was delivering 6 to 10 W at 6.345 GHz into an impedance of $(8 + j21.4)$ ohms.

may be written in terms of the Fourier components at the first and third harmonics as

$$\left.\begin{aligned}(v - V_0) &= (v_0 - V_0) + v_1 + v_1^* + v_3 + v_3^* \\ q &= q_0 + q_1 + q_1^* + q_3 + q_3^*\end{aligned}\right\}, \tag{18}$$

where the subscript and the star indicate the harmonic and the conjugate. Separating out the two harmonics and ignoring† the currents and voltage at other harmonic frequencies from the equations, we have

$$\frac{v_3}{\alpha} = (q_1^3 + 6q_1q_1^*q_3 + 3q_0^2q_3 + 3q_3^2q_3^*) \tag{19}$$

$$\frac{v_1}{\alpha} = (6q_1q_3q_3^* + 3q_0^2q_1 + 3q_1^2q_1^* + 3q_1^{*2}q_3) \tag{20}$$

$$\frac{v_0 - V_0}{\alpha} = (q_0^3 + 6q_0q_1q_1^* + 6q_0q_3q_3^*). \tag{21}$$

Further, we have the relation between the instantaneous charge q and its Fourier components

$$q_b < q = q_0 + q_1 + q_1^* + q_3 + q_3^* < 0. \tag{22}$$

If the power and impedance at the third harmonic are known, then v_3 and q_3 are known, and for various values of q_0, the values of q_1 may be computed from (19). If the varactor diode is capable of sustaining the assumed output, then the net charge q during any one cycle of oscillation at the exciting frequency should be less than the breakdown charge q_b computed from the relation

$$q_b = \sqrt[3]{(V_b - V_0)/\alpha}. \tag{23}$$

The value of V_b is known from the diode design presented in (3).

A.3.2 Lossy varactor formulations

If R_s is the series resistance of the diode, then eqs. (19) and (20) become

$$\frac{v_3 + I_3R_s}{\alpha} = q_1^3 + 6q_3|q_1|^2 + 3q_0^2q_3 + 3q_3|q_3|^2 \tag{24}$$

$$\frac{v_1 - I_1R_s}{\alpha} = 6q_1|q_3|^2 + 3q_0^2q_1 + 3q_1|q_1|^2 + 3q_3q_1^{*2}. \tag{25}$$

Equation (24) may be solved by rewriting it in terms of q_1^3 and multiplying it by q_1^{*3}, which leads to an equation in terms of $|q_1|^6$, $|q_1|^4$,

† The physical basis for ignoring the other harmonics is that the circuit presents very large impedances at these frequencies, and there is effectively no flow of current or oscillation of charge at these extraneous frequencies.

$|q_1|^2$, and a constant. This resulting equation is a cubic equation in terms of $|q_1|^2$, and only its real and positive root is a valid solution for (24).

If the computed value of q_1 which corresponds to a prechosen value of q_0 and q_3 also satisfies (22), we have the necessary condition for generation of the power P which originally resulted in q_3.

The current I_1, voltage v_1, and bias voltage v_0 are calculated from q_1, eq. (25), and eq. (21), respectively. The efficiency is known by the computation of the power dissipated because of the first and third harmonic currents and their conjugates in R_s.

REFERENCES

1. S. V. Ahamed and J. C. Irvin, "New Frontiers of Varactor Harmonic Power Generation in the C-Band," B.S.T.J., *53*, No. 9 (November 1974), pp. 1839–1843.
2. P. Penfield, Jr., and R. P. Rafuse, *Varactor Applications*, Cambridge, Mass.: M. I. T. Press, 1962.
3. A. Y. Cho and F. K. Reinhart, "Interface and Doping Profile Characteristics with Molecular Beam Epitaxy of GaAs: GaAs Voltage Varactor," J. Appl. Phys., *45*, No. 4 (April 1974), pp. 1812–1817.
4. R. A. Moline and G. F. Foxhall, "Ion-Implanted Hyperabrupt Voltage Variable Capacitors," IEEE Trans. on Electron Devices, *ED-19*, No. 2 (February 1972), pp. 267–273.
5. J. J. Chang, R. M. Ryder, and S. Schonbrun, "A Numerical Analysis of Varactor Frequency Doublers," Microwave Diode Research, Report No. 18, U. S. Army Electronics Laboratory Contract DA36-039SC89205, DA Project No. 1P6-22001-A-056, prepared by Bell Telephone Laboratories, Incorporated.
6. M. H. Norwood and E. Shatz, "Voltage Variable Capacitor Tuning: A Review," Proc. IEEE, *56*, No. 5 (May 1968), pp. 788–798.
7. Y. F. Chang, "Capacitance of P-n Junctions: Space Charge Capacitance," J. Appl. Phys., *37*, pp. 2337–2342.
8. Y. F. Chang, "The Capacitance of P-n Junctions," Solid-State Electronics, *10*, April 1967, pp. 281–287.
9. S. M. Sze and J. C. Irvin, "Resistivity, Mobility and Impurity Levels in GaAs, Ge at 300°K," in *Solid-State Electronics*, Vol. 11, New York: Pergamon Press, 1968, pp. 599–602.